BEST AVAILABLE IMAGES

Defective images within this document are accurate representations of the original documents submitted by the applicant.

Defects in the images may include (but are not limited to):

- BLACK BORDERS
- TEXT CUT OFF AT TOP, BOTTOM OR SIDES
- FADED TEXT
- ILLEGIBLE TEXT
- SKEWED/SLANTED IMAGES
- COLORED PHOTOS
- BLACK OR VERY BLACK AND WHITE DARK PHOTOS
- GRAY SCALE DOCUMENTS

IMAGES ARE BEST AVAILABLE COPY.

As rescanning documents *will not* correct images, please do not report the images to the Image Problem Mailbox.

TRANSMITTAL FORM

(to be used for all correspondence after initial filing)

Application No.	10/797,783
Filing Date	March 9, 2004
First Named Inventor	Marc Bernard
Art Unit	
Examiner Name	
Total Number of Pages in This Submission: 6	Attorney Docket Number: 15675P516

ENCLOSURES ***(check all that apply)***

- [x] Fee Transmittal Form
  - [ ] Fee Attached
- [ ] Amendment / Response
  - [ ] After Final
  - [ ] Affidavits/declaration(s)
- [ ] Extension of Time Request
- [ ] Express Abandonment Request
- [ ] Information Disclosure Statement
  - [ ] PTO/SB/08
- [x] Certified Copy of Priority Document(s)
- [ ] Response to Missing Parts/ Incomplete Application
  - [ ] Basic Filing Fee
  - [ ] Declaration/POA
  - [ ] Response to Missing Parts under 37 CFR 1.52 or 1.53
- [ ] Drawing(s)
- [ ] Licensing-related Papers
- [ ] Petition
- [ ] Petition to Convert a Provisional Application
- [ ] Power of Attorney, Revocation Change of Correspondence Address
- [ ] Terminal Disclaimer
- [ ] Request for Refund
- [ ] CD, Number of CD(s)
- [ ] After Allowance Communication to Group
- [ ] Appeal Communication to Board of Appeals and Interferences
- [ ] Appeal Communication to Group **(Appeal Notice, Brief, Reply Brief)**
- [ ] Proprietary Information
- [ ] Status Letter
- [x] Other Enclosure(s) *(please identify below):*

Request for Priority; return postcard

Remarks

SIGNATURE OF APPLICANT, ATTORNEY, OR AGENT

Firm or Individual name	Eric S. Hyman, Reg. No. 30,139 BLAKELY, SOKOLOFF, TAYLOR & ZAFMAN LLP
Signature	
Date	4/8/04

CERTIFICATE OF MAILING/TRANSMISSION

I hereby certify that this correspondence is being deposited with the United States Postal Service on the date shown below with sufficient postage as first class mail in an envelope addressed to: Commissioner for Patents, P.O. Box 1450, Alexandria, VA 22313-1450.

Typed or printed name	Melissa Stead		
Signature	Melissa Stead	Date	4-8-04

Based on PTO/SB/21 (02-04) as modified by Blakely, Sokoloff, Taylor & Zafman (wlr) 02/10/2004.
SEND TO: Commissioner for Patents, P.O. Box 1450, Alexandria, VA 22313-1450

FEE TRANSMITTAL for FY 2004

Effective 01/01/2004. Patent fees are subject to annual revision.

☐ Applicant claims small entity status. See 37 CFR 1.27.

TOTAL AMOUNT OF PAYMENT ($)

Complete if Known	
Application Number	10/797,783
Filing Date	March 9, 2004
First Named Inventor	Marc Bernard
Examiner Name	
Art Unit	
Attorney Docket No.	15675P516

METHOD OF PAYMENT *(check all that apply)*

☐ Check ☐ Credit card ☐ Money Order ☐ Other ☐ None

☒ Deposit Account

Deposit Account Number: 02-2666

Deposit Account Name: Blakely, Sokoloff, Taylor & Zafman LLP

The Commissioner is authorized to: *(check all that apply)*

☒ Charge fee(s) indicated below ☐ Credit any overpayments

☒ Charge any additional fee(s) or underpayment of fees as required under 37 CFR §§ 1.16, 1.17, 1.18 and 1.20.

☐ Charge fee(s) indicated below, **except for the filing fee** to the above-identified deposit account

FEE CALCULATION

1. BASIC FILING FEE

Large Entity Fee Code	Large Entity Fee ($)	Small Entity Fee Code	Small Entity Fee ($)	Fee Description	Fee Paid
1001	770	2001	385	Utility filing fee	
1002	340	2002	170	Design filing fee	
1003	530	2003	265	Plant filing fee	
1004	770	2004	385	Reissue filing fee	
1005	160	2005	80	Provisional filing fee	

SUBTOTAL (1) ($)

2. EXTRA CLAIM FEES

	Extra Claims		Fee from below		Fee Paid
Total Claims		- 20** =		X	=
Independent Claims		- 3 =		X	=
Multiple Dependent					=

Large Entity Fee Code	Large Entity Fee ($)	Small Entity Fee Code	Small Entity Fee ($)	Fee Description
1202	18	2202	9	Claims in excess of 20
1201	86	2201	43	Independent claims in excess of 3
1203	290	2203	145	Multiple Dependent claim, if not paid
1204	86	2204	43	**Reissue independent claims over original patent
1205	18	2205	9	**Reissue claims in excess of 20 and over original patent

SUBTOTAL (2) ($)

***or number previously paid, if greater, For Reissues, see below*

FEE CALCULATION (continued)

3. ADDITIONAL FEES

Large Entity Fee Code	Large Entity Fee ($)	Small Entity Fee Code	Small Entity Fee ($)	Fee Description	Fee Paid
1051	130	2051	65	Surcharge - late filing fee or oath	
1052	50	2052	25	Surcharge - late provisional filing fee or cover sheet.	
2053	130	2053	130	Non-English specification	
1812	2,520	1812	2,520	For filing a request for *ex parte* reexamination	
1804	920 *	1804	920 *	Requesting publication of SIR prior to Examiner action	
1805	1,840 *	1805	1,840 *	Requesting publication of SIR after Examiner action	
1251	110	2251	55	Extension for reply within first month	
1252	420	2252	210	Extension for reply within second month	
1253	950	2253	475	Extension for reply within third month	
1254	1,480	2254	740	Extension for reply within fourth month	
1255	1,210	2255	605	Extension for reply within fifth month	
1404	330	2401	165	Notice of Appeal	
1402	330	2402	165	Filing a brief in support of an appeal	
1403	290	2403	145	Request for oral hearing	
1451	1,510	2451	1,510	Petition to institute a public use proceeding	
1452	110	2452	55	Petition to revive - unavoidable	
1453	1,330	2453	665	Petition to revive - unintentional	
1501	1,330	2501	665	Utility issue fee (or reissue)	
1502	480	2502	240	Design issue fee	
1503	640	2503	320	Plant issue fee	
1460	130	2460	130	Petitions to the Commissioner	
1807	50	1807	50	Processing fee under 37 CFR 1.17(q)	
1806	180	1806	180	Submission of Information Disclosure Stmt	
8021	40	8021	40	Recording each patent assignment per property (times number of properties)	
1809	770	1809	385	Filing a submission after final rejection (37 CFR § 1.129(a))	
1810	770	2810	385	For each additional invention to be examined (37 CFR § 1.129(b))	
1801	770	2801	385	Request for Continued Examination (RCE)	
1802	900	1802	900	Request for expedited examination of a design application	
Other fee (specify)					

* Reduced by Basic Filing Fee Paid

SUBTOTAL (3) ($)

SUBMITTED BY

Complete (if applicable)

Name *(Print/Type)*	Eric S. Hyman	*Registration No. (Attorney/Agent)*	30,139	*Telephone*	(310) 207-3800
Signature				*Date*	4/8/04

Based on PTO/SB/17 (10-03) as modified by Blakely, Sokoloff, Taylor & Zafman (with 02/10/2004.
SEND TO: Commissioner for Patents, P.O. Box 1450, Alexandria, VA 22313-1450

DOCKET NO.: 15675P516

IN THE UNITED STATES PATENT AND TRADEMARK OFFICE

In re the Application of:

MARC BERNARD, ET AL.

Application No.: 10/797,783

Filed: March 09, 2004

For: **Large Spectrum Icing Conditions Detector For Optimization of Aircraft Safety**

Art Group:

Examiner:

Commissioner for Patents
P.O, Box 1450
Alexandria, VA 22313-1450

REQUEST FOR PRIORITY

Applicant respectfully requests a convention priority for the above-captioned application, namely:

COUNTRY	APPLICATION NUMBER	DATE OF FILING
Europe	03290582.0	10 March 2003

☒ A certified copy of the document is being submitted herewith.

Respectfully submitted,

Blakely, Sokoloff, Taylor & Zafman LLP

Dated: 4/8/04

Eric S. Hyman, Reg. No. 30,139

12400 Wilshire Boulevard, 7th Floor
Los Angeles, CA 90025
Telephone: (310) 207-3800

I hereby certify that this correspondence is being deposited with the United States Postal Service on the date shown below with sufficient postage as first class mail in an envelope addressed to: Commissioner for Patents, P.O. Box 1450, Alexandria, VA 22313-1450.

Melissa Stead 4-8-04

Melissa Stead *Date*

Anmeldung Nr:
Application no.: 03290582.0
Demande no:

Anmeldetag:
Date of filing: 10.03.03
Date de dépôt:

Anmelder/Applicant(s)/Demandeur(s):

Auxitrol SA
5, allée Charles Pathe
18000 Bourges
FRANCE

Bezeichnung der Erfindung/Title of the invention/Titre de l'invention:
(Falls die Bezeichnung der Erfindung nicht angegeben ist, siehe Beschreibung.
If no title is shown please refer to the description.
Si aucun titre n'est indiqué se referer à la description.)

Large spectrum icing conditions detector for optimization of aircraft safety

In Anspruch genommene Priorität(en) / Priority(ies) claimed /Priorité(s) revendiquée(s)
Staat/Tag/Aktenzeichen/State/Date/File no./Pays/Date/Numéro de dépôt:

Internationale Patentklassifikation/International Patent Classification/
Classification internationale des brevets:

B64D15/00

Am Anmeldetag benannte Vertragstaaten/Contracting states designated at date of filing/Etats contractants désignées lors du dépôt:

AT BE BG CH CY CZ DE DK EE ES FI FR GB GR HU IE IT LU MC NL
PT SE SI SK TR LI RO

LARGE SPECTRUM ICING CONDITIONS DETECTOR FOR OPTIMIZATION OF AIRCRAFT SAFETY

BACKGROUND OF THE INVENTION

Technical field

The invention relates to an ice detector and more particularly to an intrusive ice detector utilized to provide, whatever the spectrum of Liquid Water Droplet diameter, an accurate warning of ice accretion on the critical surfaces of an aircraft.

Background art

An ice detector is a sensor commonly used on aircraft to indicate the presence of icing conditions in the airflow that may result in ice accretion on the critical surfaces of the aircraft. Ice accretion on the aircraft parts like wings or engine intake degrades its aerodynamic performances and increases its mass. Consequently, the aircraft can become difficult to control, and in the worst case, it can crash.

Ice accretion occurs when the aircraft is flying through clouds that contains liquid water droplets at a temperature below the freezing limit. These droplets are called "supercooled droplets" and have a typical Median Volume Diameter (MVD) of 20µm (see Langmuir D distribution on figure 5). Droplets having a diameter superior to 50µm are also encountered (Supercooled Large Droplets).

The ice detector is classically positioned perpendicularly to the skin of the aircraft at a known

location that is selected to provide fast and accurate detection of ice accretion.

Referring to figure 1a to figure 3, said conventional ice detector 12 is constituted by an airfoil-shaped strut 8 and a sensing element 7 mounted upon said strut 8. The sensing element 7 is classically a magnetostrictive (figure 1a to figure 1d) or piezoelectric (figure 2a to figure 2d) oscillating probe (see U.S. Pat. Nos. 4,553,137; 4,570,881) which frequency oscillation is comprised between 20000 to 45000Hz. When ice accretes on the sensing element 7, mass of said sensing element 7 increases and consequently oscillation frequency decreases down to the detection threshold. The strut 8 extends from a mounting flange 9 to the sensing element 7 and allows measuring outside the boundary layer adjacent to aircraft skin. Ice detector 12 is fixed on the aircraft skin via the flange 9 with means such as bolts or screws. A housing 10 extends inside the aircraft, said housing 10 comprising electronic modules and a connector 13 for connecting said ice detector 10 to the aircraft control systems.

Classically, said sensing element 7 and said strut 8 extends in the airflow perpendicularly to the aircraft skin. In a particular configuration, as illustrated by figure 2a and figure 3, they are sloped from the vertical line relative to the aircraft skin in the direction of the airflow represented by the arrow 11. Said slope is generally included between 5° and 30° (see U.S. Pat. Nos. 4,333,004; 6,320,511) and is intended to decrease the equilibrium temperature (recovery effect), especially for improvement of detection at temperature near freezing point, and to facilitate the elimination of ice during

the de-icing, by allowing said ice to slide on the surface of said sensing element 7.

Prior art's sensing element 7 has a circular cross section with a constant diameter spanwise. Classically, the efficient measurement length is quite short (around 20mm). The strut length is adapted to position the sensing element at the characteristic nominal icing condition point.

However conventional ice detectors, as described herein, present several technical limitations, some of said limitations being exposed afterwards.

Non homogeneous distribution of the icing conditions

An aircraft in flight generates in its close environment a modification of the aerodynamic field (local pressure and velocity). Hence, any sensor positioned on the aircraft skin is subject to this modification and the measure made by said sensor is then altered by a more or less important variation. To take into account this modification, a correction operation is generally realized on the result of the measure through the use of a pre-established coefficient, which allows obtaining the real value from the read value.

Within the framework of ice accretion detection, said correction operation (installation coefficient) is particularly difficult. Indeed, due to their momentum, water droplets do not exactly follow the streamlines of the airflow and are more or less deviated by the presence of the aircraft. Consequently, there are some areas close to the aircraft where local water droplet concentration is superior to the upstream conditions. Figure 4 represents the concentration profile for two given sizes

of droplets versus distance from aircraft skin for two flight conditions. The distance of the maximum concentration (respectively d_1 and d_2) is then a function of the droplet size (respectively δ_1 and δ_2) and flight conditions (velocity, static temperature, altitude, angle of attack, side slip, etc.). Therefore the distribution of the local icing conditions is non-homogeneous.

According to the aircraft type, the position of the maximum concentration may vary by several centimeters (d'_1 and d'_2) along the aircraft orthogonal axis, depending on the diameter of the droplets encountered and the flight conditions.

Consequently, the prior art ice detectors are adapted to the detection of average icing conditions (described on JAR-FAR and EUROCAE standards), because the measure is focused at a fixed distance from the aircraft skin, but cannot integrate accurately all the icing conditions spectrum that can be crossed.

Slow accretion of small drops

One of the most difficult icing conditions to detect corresponds to the slow accretion of small drops, which have typically a diameter lower than 10 microns. Said small drops are indeed particularly sensitive to evaporation. Due to the aerodynamics of an aircraft, said evaporation is more sensitive on the leading edges, such as the surface of the sensing element of the ice detector, where the local temperature is closed to the total temperature of the flow, than on flat surfaces such as the wing extrados. On the surface of the sensitive element, said small drops tend to evaporate as they accrete.

Hence there is a risk that the quantity of ice present on the sensing element is not representative of the thickness of ice present on the other surfaces of the aircraft where evaporation phenomenon is less active. A delayed detection or even no detection of nevertheless real icing conditions could then occur.

Effect of supercooled large droplets (SLD) on ice accretion

Ice accretion on the sensing element is in particular function of the Velocity of the droplets (V_∞), the Liquid Water Content (LWC) of the airflow, the collection Efficiency (E) and the freezing fraction (η).

The collection efficiency E characterizes the proportion of liquid mass crossing the frontal projection of the sensing element and ultimately striking the sensing element. E parameter depends in particular on velocity V_∞, sensing element diameter (D) and droplet size (δ).

The freezing fraction η represents the proportion of incoming water that freezes on the element. In particular, η parameter depends on droplet size δ, velocity (V_∞), temperature (T_∞) and Liquid Water Content (LWC) of the airflow, and sensing element diameter (D).

The water freezing rate can be evaluated, at the first order, following the relation:

$$\dot{m}_{freezing} = \eta \times E \times LWC \times V_\infty \times S$$

The water mass (m) that accretes on the sensing element during an interval time τ is given by:

$$m = \dot{m}_{freezing} \times \tau$$

In the case of presence of SLD in the flow (see U.S. Pat. Nos.6,269,320), and due to the small diameter of conventional sensing element, freezing fraction η is significantly modified (important runback, pulverization of the droplet at impingement). Consequently, time required to accumulate the sufficient mass of ice to detect ice accretion is increased compared to smallest drops in the same condition. At the same time, due to the important size ratio between the droplet and the aircraft exposed parts (wings, engine intakes,...), local water freezing rates are not affected. Ice build up is then slower on the sensing element than on the aircraft critical parts. This results in a delayed information of ice accretion, which may affect aircraft control.

Consumption

Prior art ice detectors include a de-icing system, which generally consists of electrical heating cables disposed within the sensing element and within the strut.

After detection, both the strut and the sensing element are heated via the heating cables. It is effectively necessary to de-ice the detector in order to preserve the sensitivity of the system. Heating both the sensing element and the strut allows to get rid of the accumulated frost on both said sensing element and strut. A relevant measure can thus start again with all its accuracy.

However electric consumption is a particularly watched parameter on an aircraft and it is necessary to limit the average consumed power during a flight. Peaks of consumption are themselves relatively high, especially during certain critical phases of a flight such as

takeoff and icing conditions. Thus devices generating important peaks of consumption are particularly critical during certain phases of a flight.

Conventional ice detectors are based on an architecture that comprises two levels of consumption. A first level of consumption corresponds to the normal flight conditions (electronic consumption) while a second level of consumption corresponds to the de-icing phases (after ice accretion is detected). Ice detectors have to be able to realize measures with a maximal occurrence. For this purpose, the power consumed during the de-icing phases in order to be able to realize a new measure rapidly is important. Such a device requires consequently an important peak of electric power during the de-icing phases.

SUMMARY OF THE INVENTION

For the above discussed purposes concerning an accurate detection of ice accretion, the invention proposes an ice detector for detecting ice accretion on the surface of a structure subject to icing, said ice detector comprising a sensing element protruding into the airflow and supported relatively to a surface of said object by a strut upon which it is mounted, characterized in that said sensing element has an evolutionary profile along the longitudinal axis adapted to the spectral distribution of the icing conditions. Said sensing element is adapted to the profile of ice distribution on the aircraft and allows detection on a large spectrum of droplet sizes. Advantageously, some parts of said sensing element are more sensitive to small droplets when others are adapted to large droplets.

In a preferred embodiment, said strut comprises a deflector to increase the local concentration of the droplets (improvement of collection Efficiency E of the sensing element) to provide a faster detection of ice accretion and to compensate evaporation effect on small droplets.

Said ice detector provides advantageously a signal indicating the severity of the icing conditions in which said structure is immersed. The severity of the icing conditions is determined by the speed at which ice accumulate through analysis of the slope of the variation of the sensing element oscillation frequency.

Finally, in accordance with the invention, power consumption during de-icing phases of the ice detector is advantageously reduced by using a first power supply dedicated to the strut and maintained during the whole duration of icing condition detection, and by using a second power supply to de-ice the sensing element.

BRIEF DESCRIPTION OF THE DRAWINGS

Other characteristics, purposes and advantages of the invention will appear to the reading of the following detailed description, with respect to the annexed drawings, given as non restrictive examples, in which:

- Figure 1a, which has already been discussed above, represents a side view of a conventional ice detector extending perpendicularly to aircraft skin and with a constant cross section spanwise;
- Figure 1b, which has been discussed above, represents a front view, in the direction of the incident airflow, of the ice detector of figure 1a;

- Figure 1c, which has been discussed above, represents a top view of the ice detector of figure 1a;
- Figure 1d, which has been discussed above, represents a perspective view of the ice detector of figure 1a;
- Figure 2a, which has already been discussed above, represents a side view of a conventional ice detector sloped from vertical line in the direction of the flow, with constant cross section spanwise and oscillation axis perpendicular to longitudinal axis;
- Figure 2b, which has been discussed above, represents a front view, in the direction of the incident airflow, of the ice detector of figure 2a;
- Figure 2c, which has been discussed above, represents a top view of the ice detector of figure 2a;
- Figure 2d, which has been discussed above, represents a perspective view of the ice detector of figure 2a;
- Figure 3, which has already been discussed above, represents a side view of another prior art ice detector sloped from vertical line in the direction of the flow, with constant cross section spanwise;
- Figure 4 represents the concentration profile for two given sizes of droplets versus distance from aircraft skin for two flight conditions;
- Figure 5 represents Langmuir D distribution of droplet size (Median Volume Diameter MVD = 20μm);
- Figure 6 represents the operating principle of the ice detector of the invention;
- Figure 7a represents a sensing element with a circular cross section which evolutionary profile has a conical shape;

- Figure 7b represents a sensing element with a circular cross section which evolutionary profile is made of successive coaxial cylinders;
- Figure 7c is a top view of a sensing element with a an evolutionary profile which cross section is circular;
- Figure 7d is a top view of a sensing element with a an evolutionary profile which cross section is elliptic;
- Figure 7e is a top view of a sensing element with a an evolutionary profile which cross section is polygonal;
- Figure 8 represents the product of coefficient efficiency E by the freezing fraction η versus the ratio of the droplet diameter δ over the sensing element diameter D, for conventional sensing element and conical shape sensing element;
- Figure 9a represents measurement length of sensing element of figure 7a compared to conventional sensing element for a given flight condition;
- Figure 9b represents measurement length of sensing element of figure 7a compared to conventional sensing element for a different flight condition from 9a;
- Figure 10a represents a side view of a typical ice detector made according to the present invention using sensing element of figure 7a;
- Figure 10b represents a front view, in the direction of the incident airflow, of the ice detector of figure 10a;
- Figure 10c represents a top view of the ice detector of figure 10a;

- Figure 10d represents a perspective view of the ice detector of figure 10a;
- Figure 11a represents a side view of a typical ice detector made according to the present invention using sensing element of figure 7b;
- Figure 11b represents a front view, in the direction of the incident airflow, of the ice detector of figure 11a;
- Figure 11c represents a top view of the ice detector of figure 11a;
- Figure 11d represents a perspective view of the ice detector of figure 11a;
- Figure 12a represents a side view of a preferred embodiment for installation on aircraft areas with high boundary layer thickness;
- Figure 12b represents a front view, in the direction of the incident airflow, of the ice detector of figure 12a;
- Figure 12c represents a top view of the ice detector of figure 12a;
- Figure 12d represents a perspective view of the ice detector of figure 12a;
- Figure 13a represents a side view of a preferred embodiment for installation on aircraft areas with low boundary layer thickness;$
- Figure 13b represents a front view, in the direction of the incident airflow, of the ice detector of figure 13a;
- Figure 13c represents a top view of the ice detector of figure 13a;
- Figure 13d represents a perspective view of the ice detector of figure 13a;

- Figure 14a represents a rounded surface deflector implemented on the strut;
- Figure 14b represents a flat surface deflector implemented on the strut;
- Figure 15a illustrates the variation of the sensing element oscillation frequency and of its derivative according to time for different icing conditions;
- Figure 15b illustrates the influence of water freezing rate over detection time;
- Figure 15c represents absolute value of derivative of oscillation frequency versus water freezing rate;
- Figure 16a is a first electric circuitry diagram proposed for heating strut and sensing element;
- Figure 16b is a second electric circuitry diagram proposed for heating strut and sensing element;
- Figure 16c is a third electric circuitry diagram proposed for heating strut and sensing element.
- Figure 17 represents limitation of electrical consumption of the invention compared to prior art.

DESCRIPTION OF THE PREFERRED EMBODIMENT

An ice detector comprises an intrusive oscillating probe, also called sensing element, mounted on a strut, said strut length depending on the measurement point required and boundary layer thickness, and a flange supported by aircraft mounting surface, said strut being fixed to said flange and a housing which extends into the interior of the aircraft. Said housing comprises various electronic cards and components used more particularly for sensing element oscillation frequency excitation and measurement, power supply management and EMI

(ElectroMagnetic Interference)/EMC (ElectroMagnetic Compatibility) protection, and a connector for connecting said ice detector to aircraft control systems.

Operating principle

The ice detector is made of a mechanical vibratory system. The sensing element positioned in the airflow is vibrated to one of its mechanical resonance frequencies (compression mode) by the excitation portion of the circuitry. The compression mode is chosen not to be sensitive to airflow velocity, particles (sand, dust,…), rain and contaminants (fuel, oil,…). This oscillation frequency is chosen above 20000Hz not to be sensitive to aircraft vibration spectrum and is sufficiently energetic to sense ice accretion on the sensing element. As it is illustrated on figure 6, when ice comes to accumulate on said sensing element, mass of sensing element increases and consequently said oscillation frequency declines. The decline of the sensing element oscillation frequency depends on the mass of ice which deposits on said sensing element, which is a function of the Liquid Water Content (LWC) of the airflow, the Velocity of the droplets (V_∞), the freezing fraction (η) and the collection Efficiency (E) of said sensing element. To prevent temperature influence on the ice detector performances, the material used to manufacture the sensing element has an elastic modulus that is constant in temperature.

The measurement portion of the circuitry detects any decline in oscillation frequency caused by ice accretion on the surface of the sensing element. When the deposit of ice is important enough for the decline of frequency to reach and exceed a fixed threshold, the ice detector

sends a "Ice detected" signal to the icing protection system of the aircraft (figure 6).

The heating system ensures afterwards the de-icing of both sensing element and strut where ice has accumulated. Once ice is evacuated, the sensing element oscillation frequency returns to nominal value and the de-icing system is switched off. New ice accretion detection can thus begin. The "Ice detected" signal is maintained until no detection occurs during a predetermined duration (typically sixty seconds).

Adaptation to local airflow of sensing element profile

It is an objective of the invention to optimize the geometry of the sensing element according to the location on the aircraft and to icing conditions to be detected. Thus the measure is realized taking into account boundary layer thickness, profile of Liquid Water Content (LWC) distribution and spectrum of droplet size along the distance to the aircraft skin.

As it has already been stated above, the concentration of drops evolves with the distance to the aircraft skin according to the size of the drops. Figure 4 illustrates typical concentration profiles for two given sizes of drops and two flight conditions (Velocity, Temperature, Altitude,...), at the same location on the aircraft. Considering flight condition 1, for a first given size of drops (curve δ_1), the concentration is maximal at a distance d_1 from the aircraft skin whereas, for a second given size of drops (curve δ_2), the concentration is maximal at a distance d_2 from the aircraft skin. As shown on flight condition 2, distances

d_1 and d_2 are modified to respectively d'_1 and d'_2 due to modification of the flow.

Conventional ice detectors are classically constituted of a cylindrical sensing element with constant circular section. Dimensions of said sensing element result from a compromise between sensitivity to ice accretion, value of oscillation frequency, mechanical resistance, sensitivity to environmental conditions (airflow velocity, aircraft vibrations, particles,...). In consequence, due to constant circular cross section spanwise, the sensing element length is relatively short (around 20mm) to preserve a sufficient rigidity. In this configuration, the measurement point is defined according to the maximal concentration average distance and said sensing element is positioned, thanks to strut length, at the distance required. The measure is thus adapted for medium droplet size.

The invention proposes to improve ice detection in terms of distance range of measurement and spectrum of droplet sizes by using a sensing element that is characterized by an evolutionary profile.

Figures 7a, 7b, 7c, 7d and 7e show views of a sensing element with different evolutionary profiles. Said sensing element extends on a substantial length, generally ranging between 45 to 65 millimeters.

Figure 7a shows a sensing element 7a, which has a substantially conical shape. Thus, the sensing element circular cross section (figure 7a) presents a diameter that decreases continuously with the increase of the distance to the aircraft skin. The base of said sensing element 7a has the largest diameter D_{Max} while tip of said sensing element 7a has the smallest diameter D_{min}.

Diameter D_{Max} is about 10 millimeters while diameter D_{min} is about 2 millimeters.

As stated before, ice accretion on the sensing element is, in particular, characterized by collection efficiency E and freezing fraction η. Classically, at fixed flight conditions, E parameter is proportional to droplet diameter δ and inversely proportional to sensing element diameter D: $E = function\left(\delta, 1/D\right)$. Consequently, at fixed droplet diameter δ, E parameter decreases from tip to base of conical sensing element. At a fixed point of sensing element, E parameter increases with droplet diameter δ.

η parameter is typically proportional to sensing element diameter D and inversely proportional to droplet diameter δ: $\eta = function\left(D, 1/\delta\right)$. Thus, at fixed droplet diameter δ, η parameter increases from tip to base of the conical sensing element. At a fixed point of the sensing element, η parameter decreases with droplet diameter δ.

Consequently, at fixed flight conditions, value of $E \times \eta$ is conserved along longitudinal axis for a sensing element with conical shape. Considering conventional sensing elements, value of $E \times \eta$ is not conserved along longitudinal axis due to constant diameter. This is illustrated on figure 8: for the median ratio of the droplet diameter δ over the sensing element diameter D, $E \times \eta$ value is the same for both sensing elements. Considering δ/D ratios inferior to median value, $E \times \eta$ value of conventional sensing element decreases whereas $E \times \eta$ value of sensing element of the invention is

conserved. The same effect is observed for δ/D ratios superior to median value. Consequently, accuracy of ice accretion detection is conserved whatever the droplet diameter for an ice detector of the invention contrary to conventional ice detectors.

As stated herein, different accumulation zones are defined along said sensing element 7a, the transition between said accumulation zones being continuous. On classical installation areas on aircraft, maximum concentration of large droplets is met close to aircraft skin whereas maximum concentration of small droplets is met further from aircraft skin. Thus, large droplets tend to accumulate on a portion of said sensing element 7a which has a large diameter while small drops tend to accumulate on a portion of said sensing element 7a which has a small diameter. Or, as it has already been demonstrated above, $E \times \eta$ value is maximum at the tip of said sensing element considering small droplets and $E \times \eta$ value is maximum at the base of said sensing element considering large droplets. Therefore, ice accretion is optimal along longitudinal axis and thus the measurement integrates advantageously the whole distribution of water droplets present in the airflow.

Another advantage of the conical shape is to obtain a longer sensing element than conventional sensing element (length ratio ranging between 2 to 3) while preserving an oscillation frequency above 20000Hz and the sensitivity to ice accretion. At the same time, insensitivity to environmental conditions (such as aircraft vibration, sand and airflow velocity) is

preserved. Consequently, the measurement length can be adapted to the whole local icing conditions in terms of droplet size and flight conditions. This is illustrated on figure 9a and figure 9b for two flight conditions. On said conventional ice detector, due to the limited measurement length, only a fraction of the local maximum of concentration is recovered by the sensing element if said maximum of concentration is not centered on the sensing element. Considering the ice detector of the invention, a maximum of local concentration is recovered by the sensing element whatever the flight condition. Consequently, the accuracy of the ice detector of the invention is conserved on the flight envelope.

Figure 7b presents a sensing element 7b that is substantially constituted by different successive coaxial cylinders, diameters of said cylinders decreasing with the increase of the distance from aircraft skin. Thus, the sensing element circular cross section has a diameter that decreases discontinuously with the increase of the distance from the aircraft skin. The sensing element 7b represented on figure 7b is made of three cylindrical portions. A first cylindrical portion, positioned at the base of said sensing element 7b, has the largest diameter D_1. A second cylindrical portion prolongs said sensing element 7b and presents a diameter D_2 smaller than D_1. A third cylindrical portion prolongs said sensing element 7b and constitutes said sensing element tip portion. The diameter of said third cylindrical portion D_3 is smaller than D_2 and hence than D_1. Diameter D_1 is about 10 millimeters while diameter D_2 is about 6 millimeters and diameter D_3 about 2 millimeters. Said three cylindrical portions define three different ice accumulation zones

onto said sensing element 7b. Schematically, the first cylindrical portion (diameter D_1) is adapted for the accumulation of large drops, the second cylindrical portion (diameter $D_2<D_1$) is adapted for the accumulation of medium sized drops and the third cylindrical portion (diameter $D_3<D_2<D_1$) is adapted for the accumulation of small drops. As for the conical sensing element 7a illustrated on figure 7a, said sensing element 7b shape allows obtaining a longer sensing element than a conventional sensing element. Number of coaxial cylinders, as presented herein, is non-restrictive and can be advantageously adapted as it is exposed hereafter.

A particular advantage of said sensing element made of coaxial cylinders, is to have a dedicated oscillation frequency for each cylinder. This allows determining the diameter of droplets that strike the sensing element. Indeed, as stated before, $Ex\eta$ value of a cylinder characterized by its diameter D is maximum for a given droplet diameter δ, at fixed flight conditions. Using coaxial cylinders with different diameters, it is possible to segregate the spectrum droplet diameter δ in dedicated intervals. For example, on sensing element of figure 7b, diameter D_1 is dedicated to detect accretion of droplets characterized by a diameter comprised in an interval centered on diameter δ_1, diameter D_2 is dedicated to detect accretion of droplets characterized by a diameter comprised in an interval centered on diameter δ_2 and diameter D_3 is dedicated to detect accretion of droplets characterized by a diameter comprised in an interval centered on diameter δ_3.

As specified before, number of coaxial cylinders is non-restrictive and precision of droplet diameter is increased by using a more important number of coaxial cylinders. The knowledge of the main diameter of droplets is a major advantage concerning ice protection systems of the aircraft. Indeed, when only small droplets are encountered, it is not necessary to switch on the ice protection system immediately because of slow or no accretion on aircraft parts. Conversely, Super Large Droplets need to be detected to provide an efficient de-icing of the aircraft part subject to icing. Consequently, the ice detector of the invention improves flight safety.

Taking into account the installation area and flight condition, the proportion of Liquid Water Content of each size can be measured with an appropriate treatment.

According to the measuring principles describe herein, the cross section of the sensing element of the invention is not necessary circular. As it is illustrated on figure 7d and 7e, the cross section of the sensing element may have also a polygonal or elliptic shape.

In a classical assembly type (figure 10a to figure 11d), the sensing element with an evolutionary profile (7a, 7b) is mounted on a strut, which length is adapted to boundary layer thickness at the installation point, perpendicularly to aircraft skin and flow direction.

Figures 12a to 13d illustrate a preferred embodiment wherein said sensing element is sloped from the vertical line relative to the aircraft skin in the direction of the airflow to optimize detection of small droplets. Indeed, as it has been stated above, said small droplets are particularly sensitive to evaporation due to

conversion of kinetic energy to temperature at impact point. Due to evolutionary profile and slope of the sensing element, a longitudinal velocity component appears and allows reducing conversion of kinetic energy into temperature. As temperature of small droplets is lower, evaporation is limited and thus detection is more accurate. Advantageously, the slope of the sensing element allows increasing the accretion area compared to the projected surface. Consequently, ice build up is facilitated on the sensing element. Said slope is generally included between 5° and 35°.

As a conclusion, the ice detectors of the invention offer a number of parameters such as strut length, sensing element profile, diameter and length, slope angle which can be advantageously customized to provide an accurate detection of ice accretion, taking into account aircraft type, installation area and icing conditions encountered.

Increase of local concentration on sensing element by adjunction of a deflector on the strut

Conventional struts have an airfoil shape, which reduces the drag of the ice detector. The face adjacent to the sensing element is classically perpendicular to the strut axis, i.e. parallel to airflow direction. This conventional embodiment does not influence the local concentration of droplets that strike the sensing element. The invention proposes the implementation of a deflector on the strut of the ice detector to increase local concentration of droplets that deposit on the sensing element, advantageously concerning small droplets. This allows improving the collection Efficiency

E of the sensing element that results in a faster detection of ice accretion.

Said deflector is oriented so that streamlines are locally deflected in the direction of the sensing element. Therefore, droplets that should have struck the strut on conventional ice detectors are guided towards the sensing element. The efficiency of the deflector depends on the momentum of supercooled water droplets.

Figures 14a and 14b illustrate respectively such an integration of a deflector 14a, 14b on a strut upon which a sensing element is mounted. The strut has a classical airfoil or elliptical shape. Figure 14a represents a strut upon which a rounded concave surface deflector 14a is set up, the roundness of said deflector 14a being steered inward said strut. Figure 14b represents a strut upon which a flat surface deflector 14b is set up.

Following the type of deflector used on said strut, increase of droplet concentration is up to 20% for small droplets and 5% for large droplets. Advantageously, and particularly concerning small droplets, evaporation effect is significantly reduced at the impact point of the sensing element due to increase of water mass flow.

Analysis of severity of ice accretion

On conventional ice detectors, severity of ice accretion is classically given by counting the number of successive detection cycles during a predetermined time.

The speed at which ice accretion occurs is a particularly relevant information characterizing the severity of the icing conditions. As it has already been stated above, when ice builds up on the sensing element, said sensing element oscillation frequency declines. The

invention proposes to use the variation of the sensing element oscillation frequency during a given time to indicate the severity of the icing conditions.

Figure 15a and 15b represent variations versus time of the sensing element oscillation frequency f for two water freezing rates Q_1 and Q_2, said water freezing rate Q_2 being more important than said water freezing rate Q_1. Considering figure 15b, at t_0 sensing element oscillation frequency is equal to nominal oscillation frequency f_{start}. Time t_1 (respectively t_2) is the time at which oscillation frequency is equal to detection threshold for condition Q_1 (respectively Q_2). As Q_2 is superior to Q_1, t_2 is inferior to t_1, due to faster accretion on the sensing element.

Therefore, by analyzing the variation of the sensing element oscillation frequency f during a given time, it is possible to obtain the mass of ice that deposits by unit of time on said sensing element and consequently on the other parts of the aircraft which are exposed to the airflow.

As it has already been stated before, the water freezing rate Q can be evaluated, at the first order, following the relation:

$$Q=\eta \times E \times LWC \times V_\infty \times S ,$$

where E is the collection Efficiency of the sensing element;

η is the freezing fraction;

S is the reference surface (m^2);

LWC is the Liquid Water Content (kg/m^3);

V_∞ is the upstream velocity of airflow (m/s).

Oscillation frequency f(t) of the sensing element can be expressed as a function of the sensing element mass m(t) as follows : $f(t)=\frac{A}{\sqrt{m(t)}}$

A is a constant depending on the material and the geometry.

The derivative versus time t of oscillation frequency f is given by: $\frac{df(t)}{dt}=-\frac{A}{2\times m(t)\times\sqrt{m(t)}}\times\frac{dm(t)}{dt}$

Mass m(t) of sensing element at time t is :

$$m(t)=m_0+m_{ice}(t)$$

m_0 is the mass of sensing element free of ice;
$m_{ice}(t)$ is the mass of ice accumulated on said sensing element ($\frac{dm_{ice}(t)}{dt}=Q$).

Assuming that $m_{ice}(t)$ is negligible compared to m_0, the derivative of oscillation frequency f is finally given by: $\frac{df(t)}{dt}=-\frac{A}{2\times m_0\times\sqrt{m_0}}\times Q=-\frac{f_0}{2\times m_0}\times Q$

where f_0 is the oscillation frequency of the sensing element free of ice.

Figure 15c represents variations of the absolute value of derivative $\frac{df}{dt}$ in function of Q: a large derivative value indicates a large value of water freezing rate Q and consequently a severe icing condition that corresponds to a quick ice accretion on the aircraft exposed parts.

Thus, the ice detector of the invention provides information of severity of icing conditions, obtained from analysis of the slope of the curve representing temporal variations of said sensing element oscillation

frequency, to aircraft protection systems for a more efficient prevention of ice accretion.

Utilizing the sensing element made of coaxial cylinders described herein, the severity of the icing conditions can be correlated to the droplet size to provide an accurate characterization of the icing environment.

Optimization of de-icing system consumption

Classically, once ice accretion has been detected by the ice detector, it is necessary to de-ice said ice detector before starting a new measurement cycle. Due to important thermal inertia of the strut and the sensing element, an important electrical power is required to de-ice the ice detector in a reduced time. According to prior art, the operating principle of the de-icing device is binary, i.e. power is maintained at a maximum value (classically 260W) during the de-icing phase and to a minimum value during the remainder of the time (<10W).

It is another objective of the invention to limit the power consumption of the ice detector during said de-icing phases by using a double de-icing command. After first detection, both strut and sensing element are de-iced via electrical heaters. When the oscillation frequency returns to nominal value, said sensing element heater is powered off whereas strut heater remains powered on. Consequently, the strut is protected from ice accretion (anti-icing mode) while ice accretion on the sensing element is detected. Supply to the strut is then stopped at the end of the alarm signal. Advantageously, the power required to avoid ice accretion is inferior to the power needed to remove the ice cap on the strut.

Therefore, peaks of consumption of an ice detector of the invention are inferior to those generated by conventional ice detectors. Power consumption can be segregated in three distinct phases as it is illustrated on figure 17): minimum power P_{min} (<10W) when no detection occurs, maximum power P'_{max} (about 200W) during de-icing phases of the sensing element and medium power P'_{medium} (about 130W) during ice accretion on the sensing element (after first detection). Advantageously, as the strut does not require being de-iced, the interval time between two consecutive detection phases of ice accretion is significantly reduced to a minimum, thus improving the accuracy of said ice detector.

In a first embodiment, this de-icing and anti-icing system is realized by using two independent electrical circuits (heater with specific power supply), one dedicated to the strut and the other one to the sensing element, each circuit being supplied by on board electrical voltage (28Vdc or 115Vac/400Hz).

In other embodiments, the invention advantageously proposes to realize this function by using only one electrical circuitry represented by the electrical diagram of figure 16a, figure 16b or figure 16c.

Figure 16a represents an electric diagram comprising three resistances. Two resistances $R_{sensing\_element}$ and R_{strut1}, mounted in parallel, are serially connected with a third resistance R_{strut2} between the potentials V_a and V_b of the power supply. Resistance $R_{sensing\_element}$ allows de-icing the sensing element whereas resistances R_{strut1} and R_{strut2} allow de-icing the strut. A switch I is disposed on the branch of the parallel circuitry which comprises said resistance $R_{sensing\_element}$. As stated above, maximum power consumption

(de-icing of sensing element) is obtained when said switch I is closed, medium power consumption is obtained when said switch I is open and minimum power consumption when system is not supplied.

Figure 16b represents a variant of electrical circuitry described herein. A resistance R'_{strut1} is mounted in parallel with two serially connected resistances $R'_{sensing\_element}$ and R'_{strut2} between the potentials V'_a and V'_b of the power supply. A switch I' is disposed on the branch of the parallel circuitry which comprises said resistances $R'_{sensing\_element}$ and R'_{strut2}. When I' is closed, said ice detector is at the maximum rated power and when I' is open medium power consumption is obtained.

Figure 16c represents another variant of electrical circuitry described herein. A resistance R''_{strut2} is either serially connected with a resistance $R''_{sensing\_element}$ or serially connected with a resistance R''_{strut1} between the potentials V''_a and V''_b of the power supply. The serial connection of said resistance R''_{strut2} with either said resistance $R''_{sensing\_element}$ or said resistance R''_{strut1} is realized thanks to a switch I''. When I'' is pointed to $R''_{sensing\_element}$, said ice detector is at the maximum rated power and when I'' is pointed to R''_{strut1}, medium power consumption is obtained.

Considering all the electrical circuits described herein, a complementary electrical resistance is used in the strut to limit power consumption between two de-icing phases of the sensing element.

CLAIMS

1. An ice detector for detecting ice accretion on a surface of a structure subject to icing, said ice detector comprising a sensing element protruding into the airflow and supported relatively to a surface of said structure by a strut upon which it is mounted, characterized in that said sensing element has an evolutionary profile, with a cross-section varying along the longitudinal axis of said sensing element, adapted to enlarge the measurement range of icing conditions, in particular in terms of droplet size spectrum and measurement length.

2. The ice detector of claim 1 further characterized in that said sensing element has a circular or elliptic cross-section.

3. The ice detector of claim 1 further characterized in that said sensing element has a polygonal cross-section.

4. The ice detector of claim 2 or 3 further characterized in that the characteristic dimension of the sensing element cross-section decreases continuously as the distance from said structure subject to icing increases.

5. The ice detector of claims 2, 3 or 4 further characterized in that said sensing element has a substantially conical shape.

6. The ice detector of claim 2 or 3 further characterized in that the characteristic dimension of the sensing element cross-section decreases discontinuously as the distance from said structure subject to icing increases.

7. The ice detector of claim 2, 3 or 6 further characterized in that said sensing element is constituted by successive coaxial cylinders adapted to identify the icing conditions encountered, particularly in terms of droplet size and concentration.

8. The ice detector of any of the preceding claims further characterized in that said sensing element is sloped, in the direction of the airflow, from the orthogonal axis of the surface upon which said ice detector is mounted.

9. An ice detector for detecting ice accretion on a surface of a structure subject to icing, said ice detector comprising a sensing element protruding into the airflow and supported relatively to a surface of said structure by a strut upon which it is mounted, characterized in that said strut comprises a deflector installed in front of said sensing element and adapted to increase the quantity of water droplets that accretes on said sensing element by locally deflecting the streamlines towards this one.

10. The ice detector of claim 9, further characterized in that said deflector is a flat surface on the strut sloped from airflow direction toward said sensing element.

11. The ice detector of claim 9, further characterized in that said deflector is a rounded concave surface on the strut sloped from airflow direction toward said sensing element.

12. An ice detector for detecting ice accretion on a surface of a structure subject to icing, said ice detector comprising a sensing element protruding into

the airflow and supported relatively to a surface of said structure by a strut upon which it is mounted, characterized in that said ice detector provides a signal indicating the severity of the icing conditions determined by the speed at which ice accretes on said sensing element trough the analysis of the slope of the curve representing the decline of the sensing element oscillation frequency over time.

13. An ice detector for detecting ice accretion on a surface of a structure subject to icing and providing an alarm signal when a substantial ice accretion is detected, said ice detector comprising a sensing element protruding into the airflow and supported relatively to a surface of said structure by a strut upon which it is mounted, said sensing element and said strut being de-iced after the detection of a substantial ice accretion, characterized in that the de-icing of said sensing element is maintained until said sensing element is free of ice whereas the de-icing of said strut is maintained during the whole duration of said alarm signal.

14. The ice detector of claim 13 further characterized in that a first power supply is dedicated specifically to the de-icing of said strut and a second power supply is dedicated specifically to the de-icing of said sensing element.

15. The ice detector of claim 13 further characterized in that a power supply is dedicated to the de-icing of both said strut and sensing element, a switch allowing heating of either both said strut and sensing element or only said strut.

PATENT OF INVENTION

LARGE SPECTRUM ICING CONDITIONS DETECTOR FOR OPTIMIZATION OF AIRCRAFT SAFETY

Applicant: AUXITROL SA (FR)

Inventor(s):

ABSTRACT

The invention proposes an ice detector for detecting ice accretion on the surface of a structure subject to icing, said ice detector comprising a sensing element protruding into the airflow and supported relatively to a surface of said object by a strut upon which it is mounted, characterized in that said sensing element has an evolutionary profile along the longitudinal axis adapted to the spectral distribution of the icing conditions. Said sensing element is adapted to the profile of ice distribution on the aircraft and allows detection on a large spectrum of droplet sizes.

In a preferred embodiment, said strut comprises a deflector to increase the local concentration of the droplets to provide a faster detection of ice accretion and to compensate evaporation effect on small droplets.

Said ice detector provides advantageously a signal indicating the severity of the icing conditions in which said structure is immersed, said severity of the icing conditions being determined by the speed at which ice

accumulates through analysis of the slope of the variation of the sensing element oscillation frequency.

Power consumption during de-icing phases of the ice detector is advantageously reduced by using a first power supply dedicated to the strut and maintained during the whole duration of icing condition detection, and by using a second power supply to de-ice the sensing element.

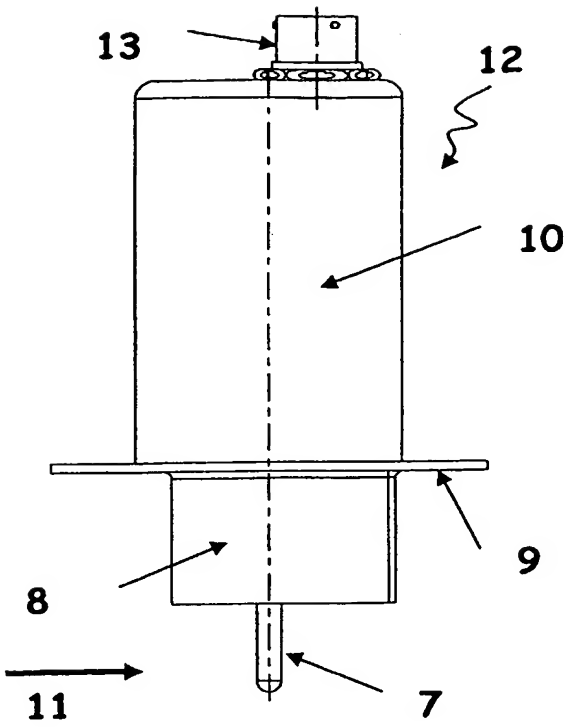

Figure 1a

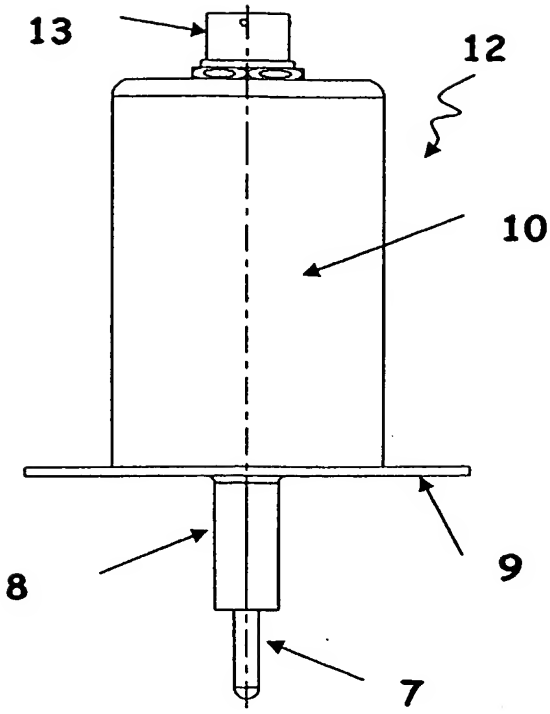

Figure 1b

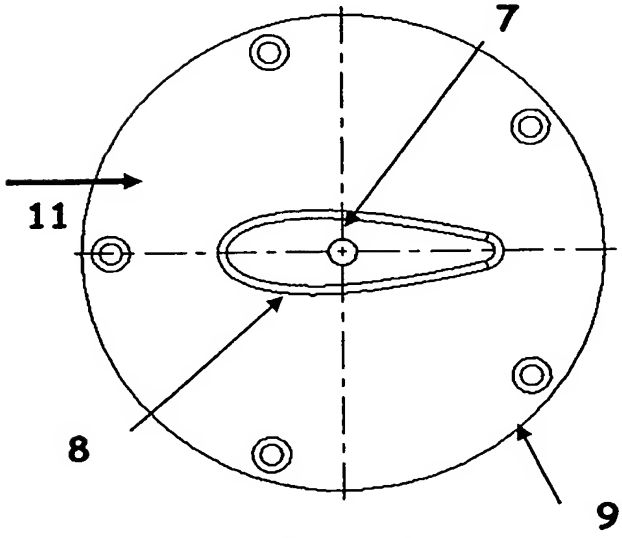

Figure 1c

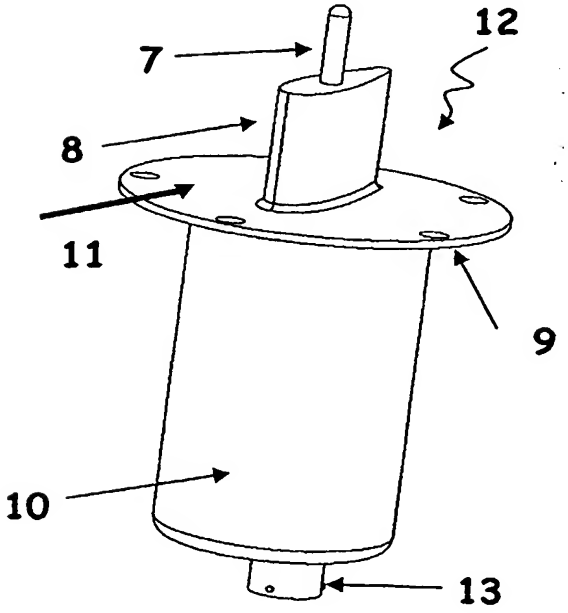

Figure 1d

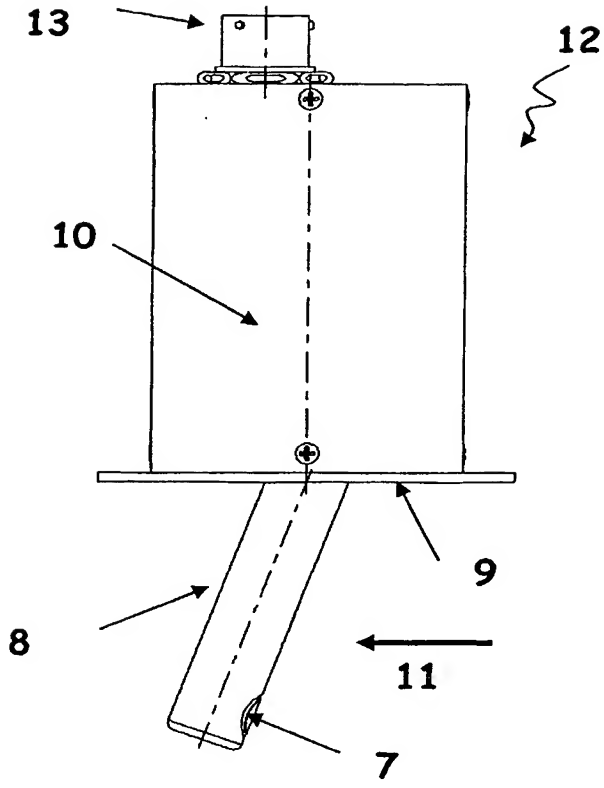

Figure 2a

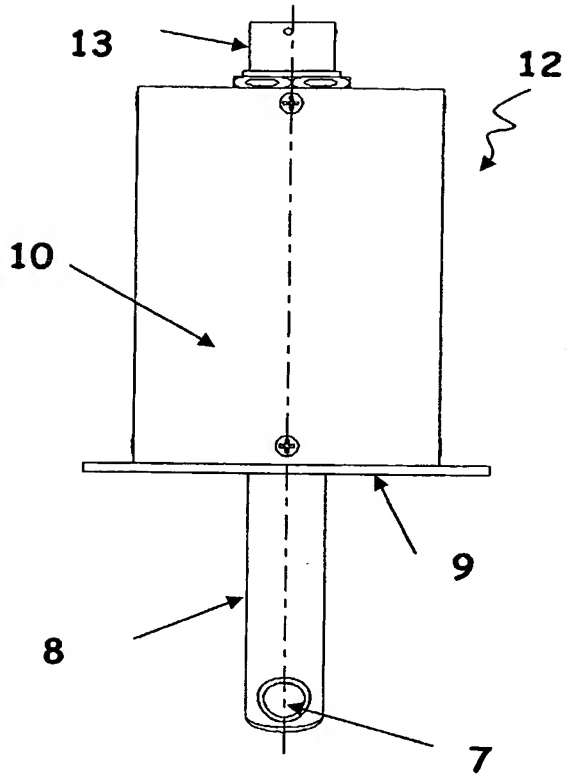

Figure 2b

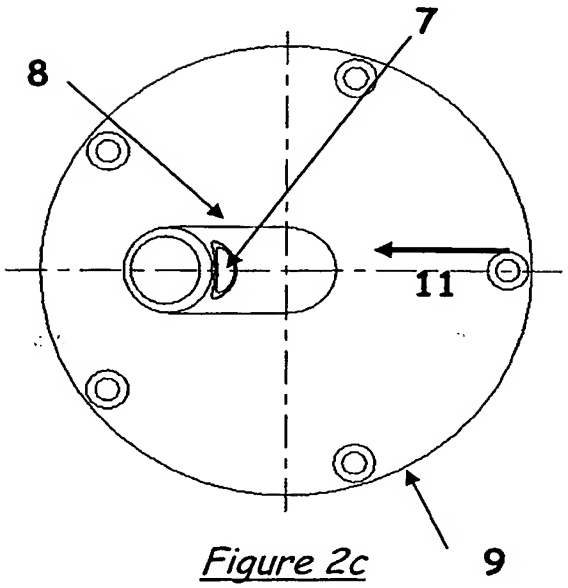

Figure 2c

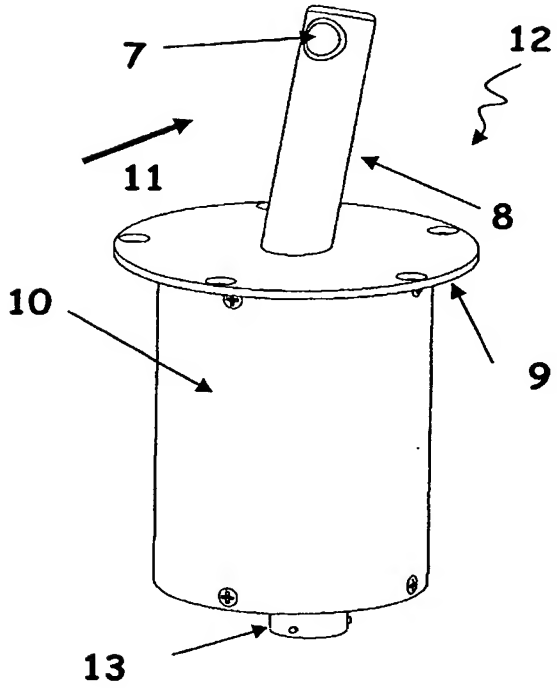

Figure 2d

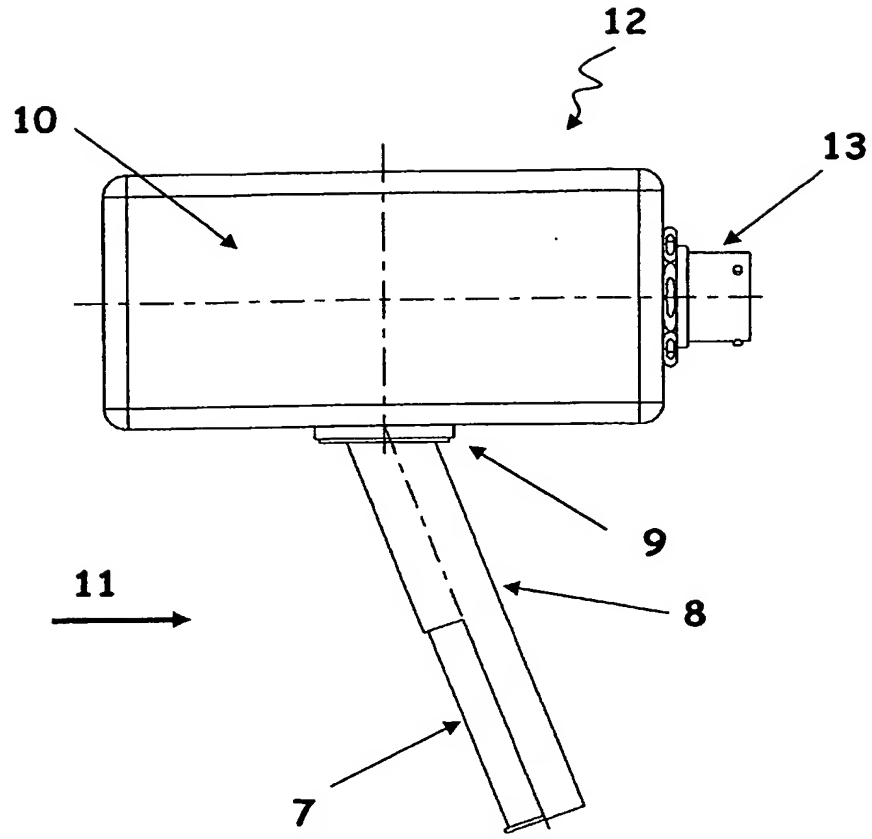

Figure 3

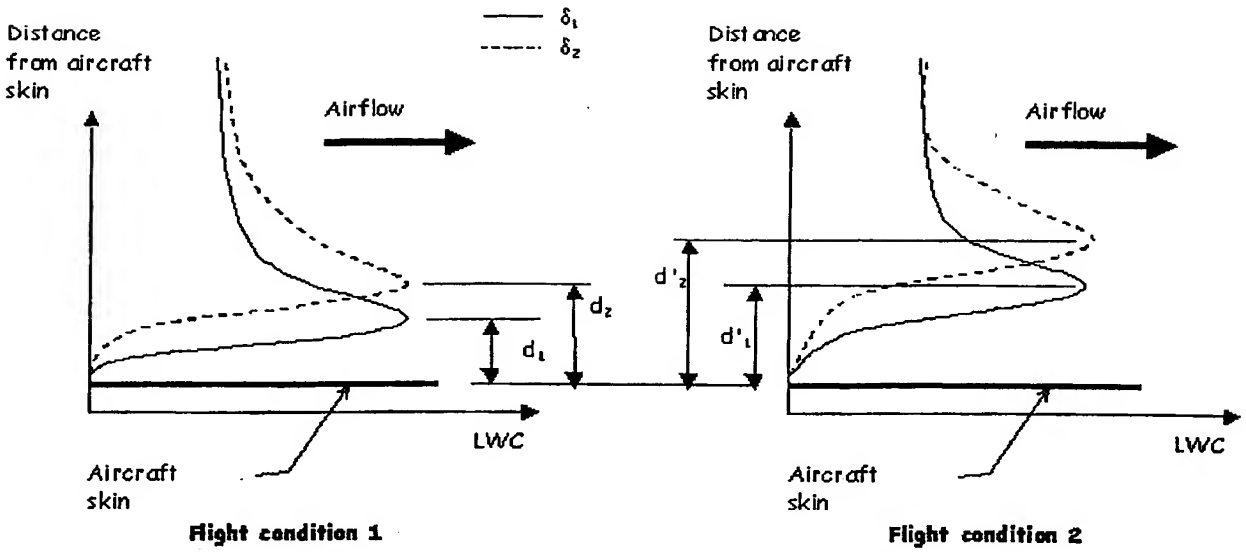

Figure 4

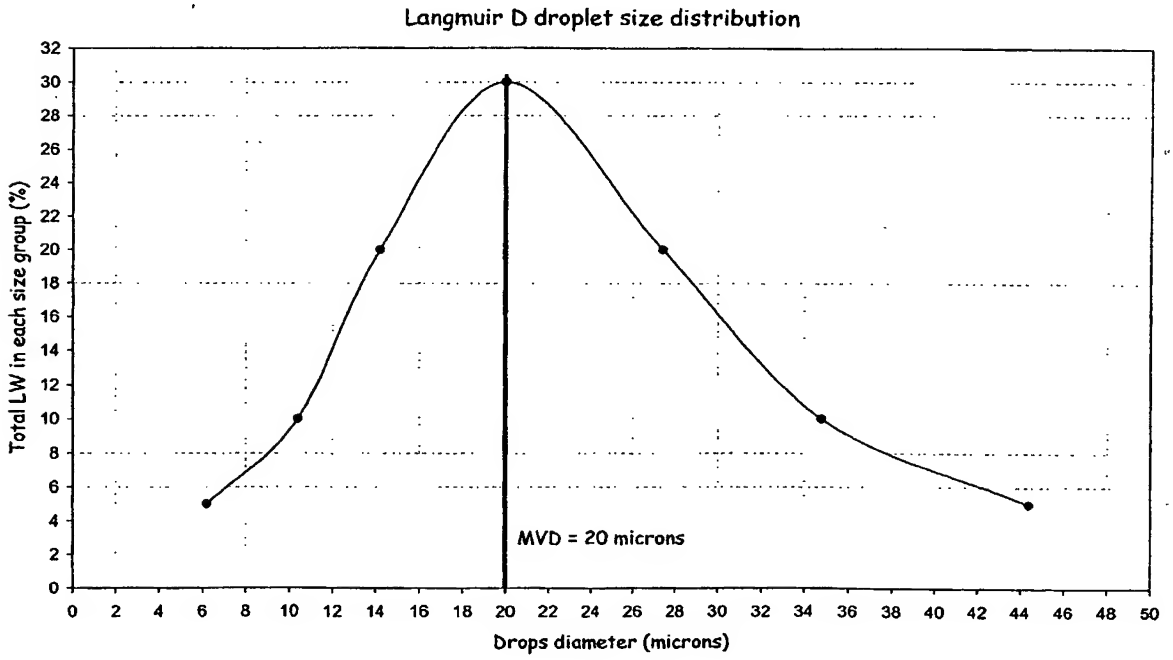

Figure 5

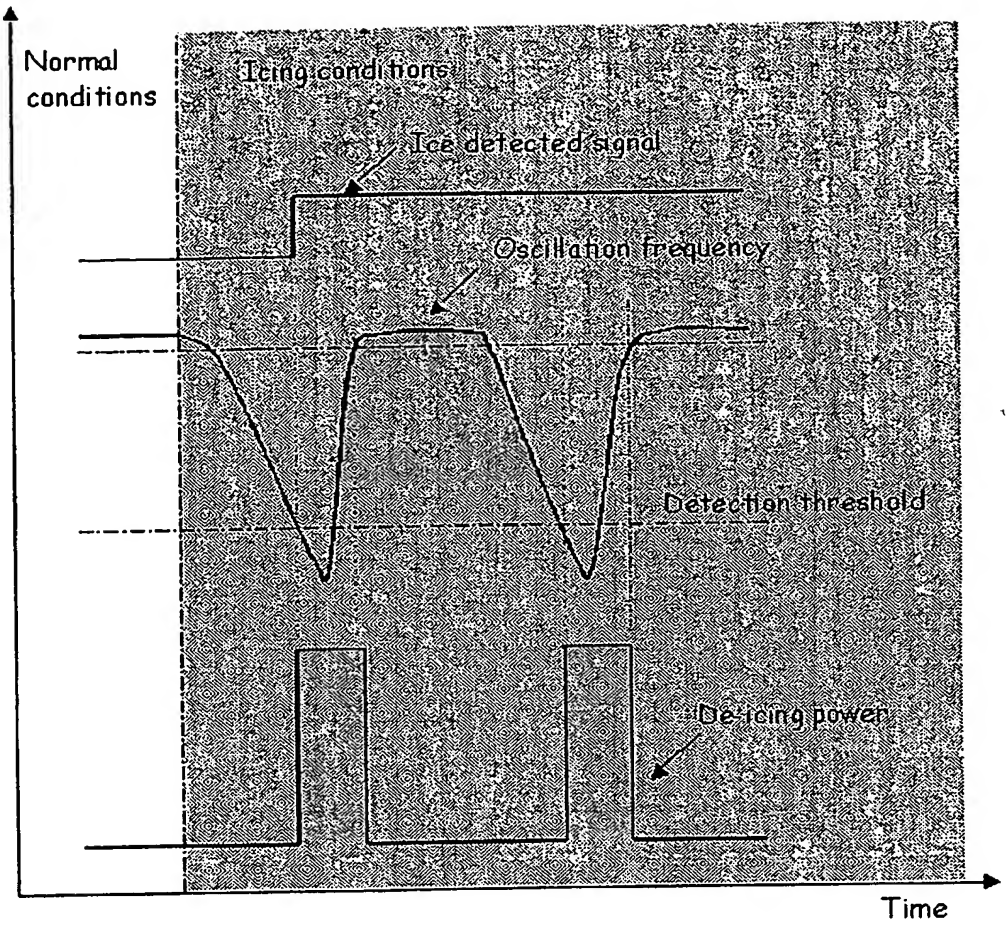
Normal conditions
Icing conditions
Ice detected signal
Oscillation frequency
Detection threshold
De-icing power
Time

Figure 6

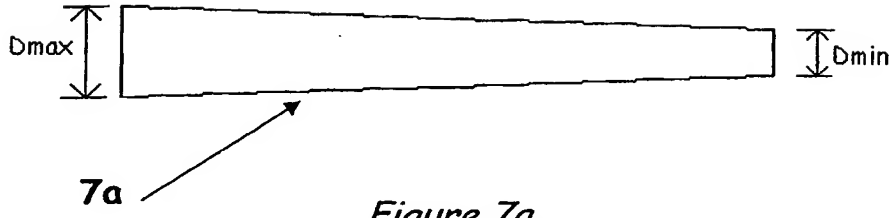

Figure 7a

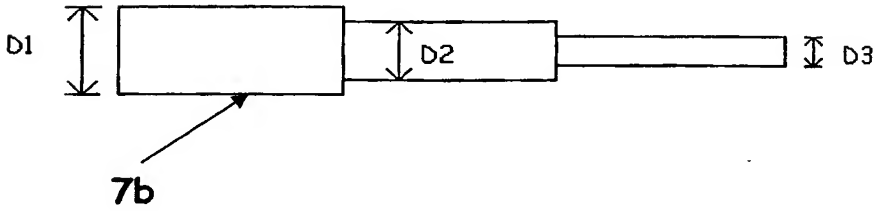

Figure 7b

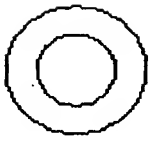

Figure 7c

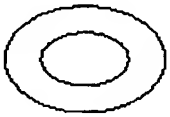

Figure 7e

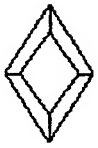

Figure 7d

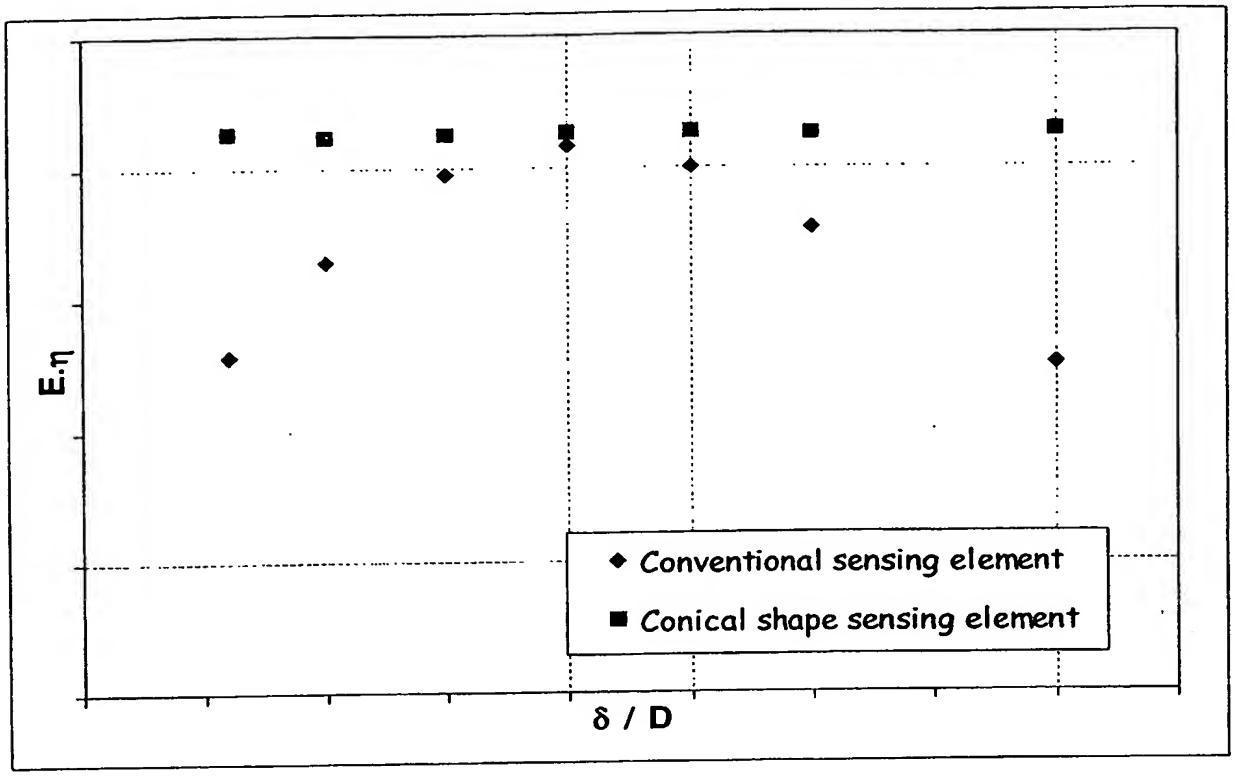
E.η
δ / D
Conventional sensing element
Conical shape sensing element

Figure 8

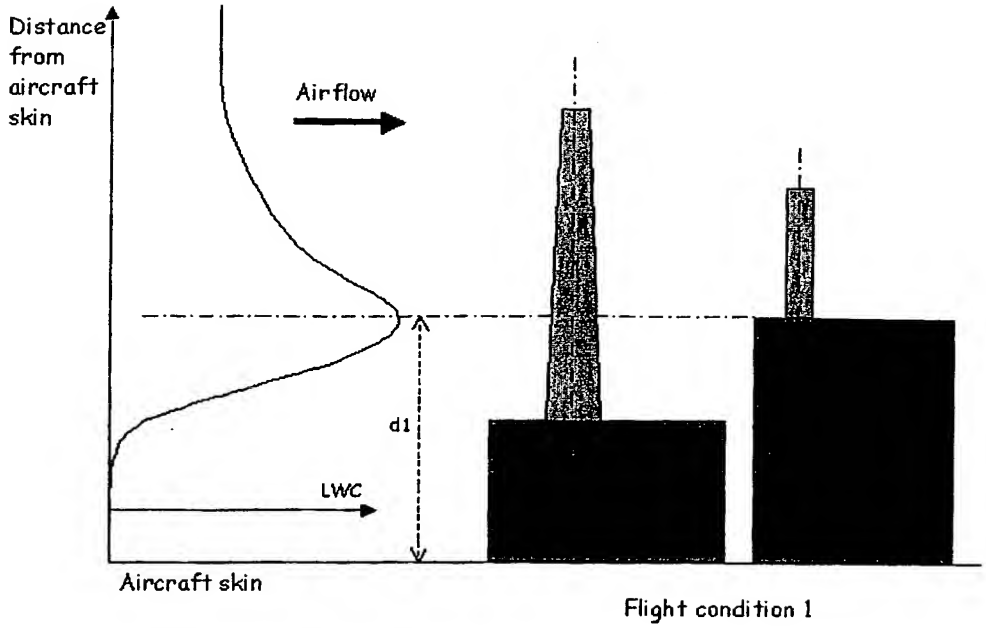

Figure 9a

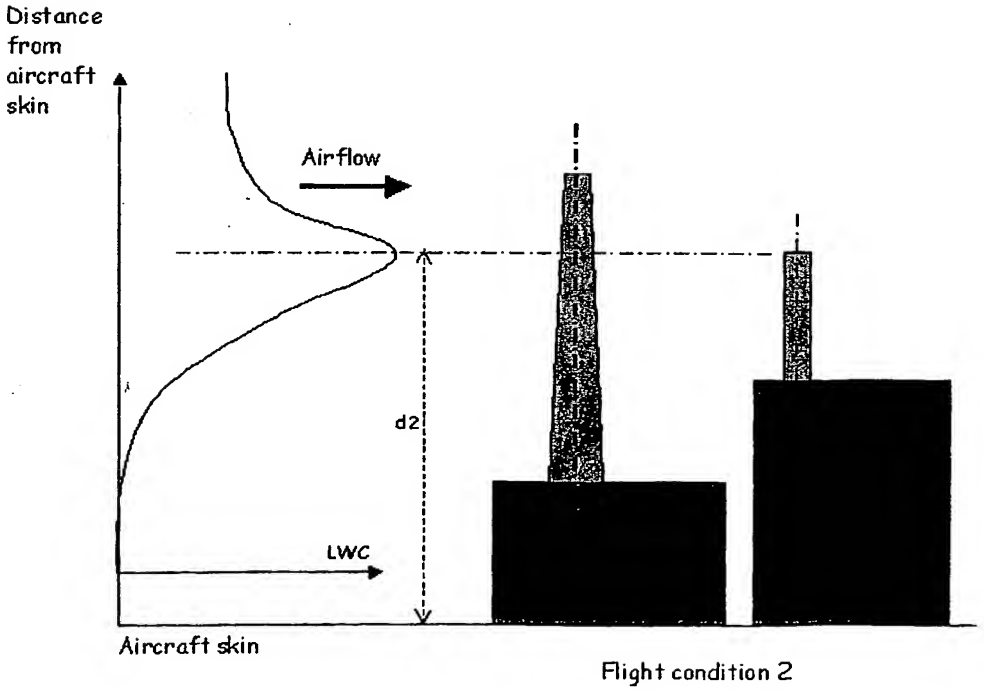

Figure 9b

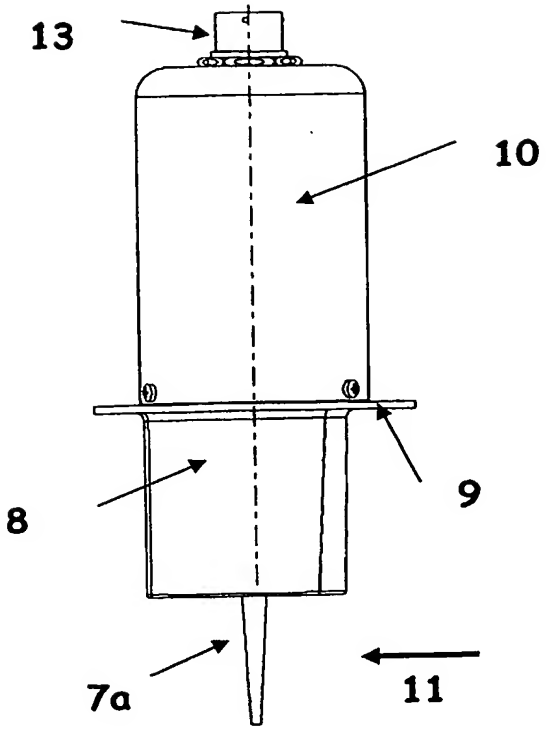

Figure 10a

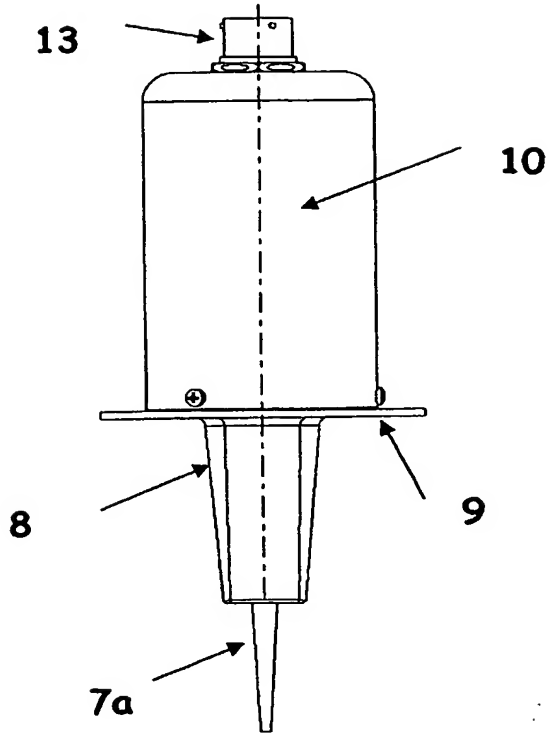

Figure 10b

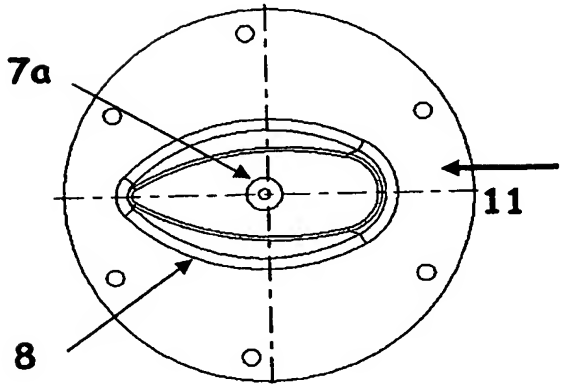

Figure 10c

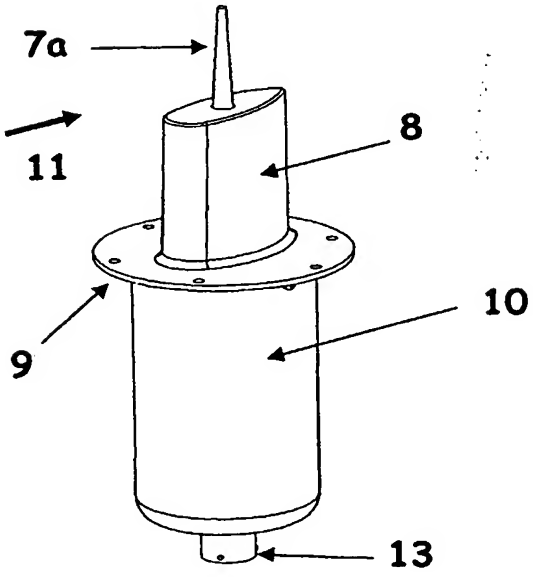

Figure 10d

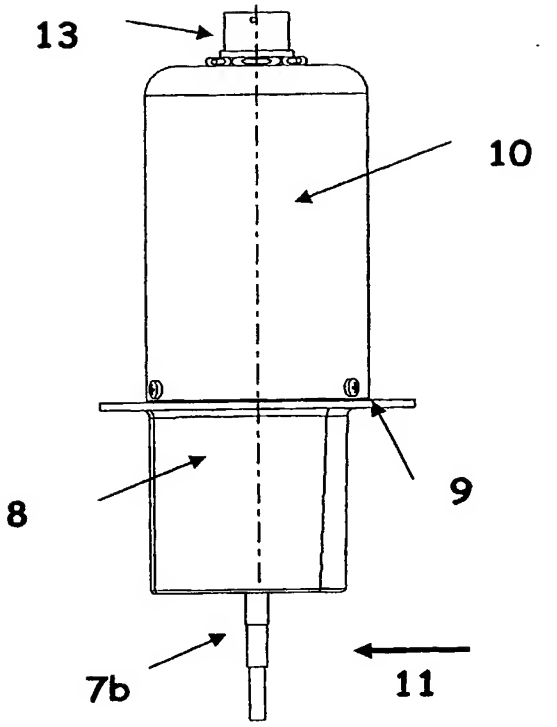

Figure 11a

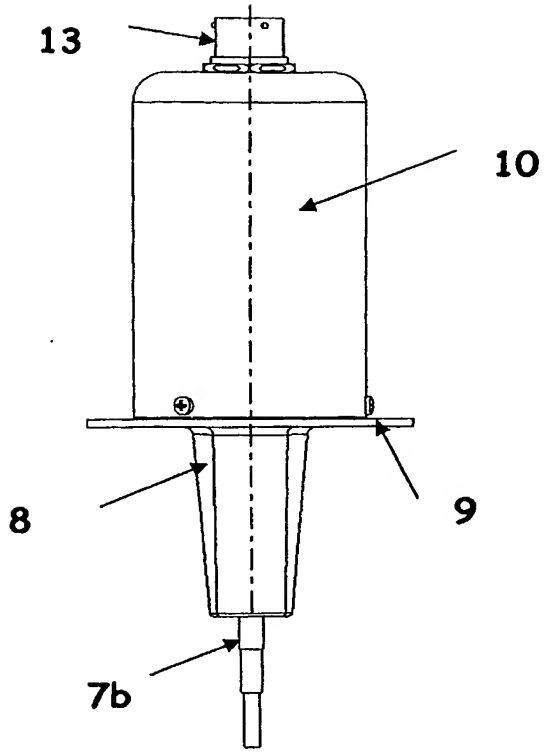

Figure 11b

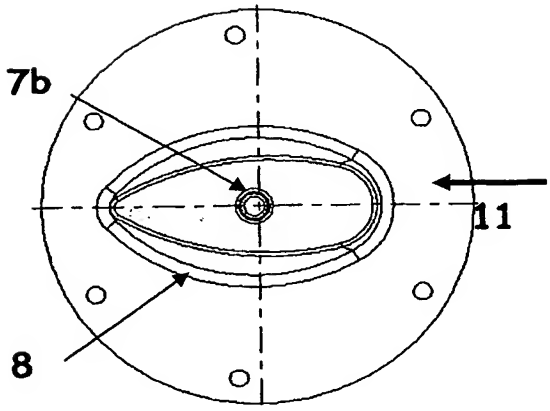

Figure 11c

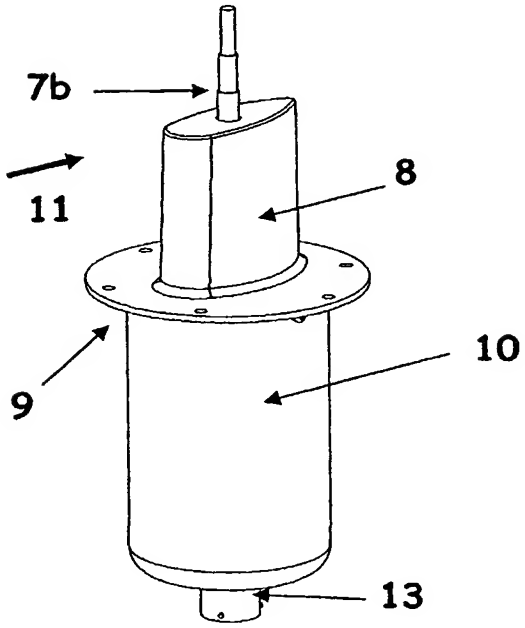

Figure 11d

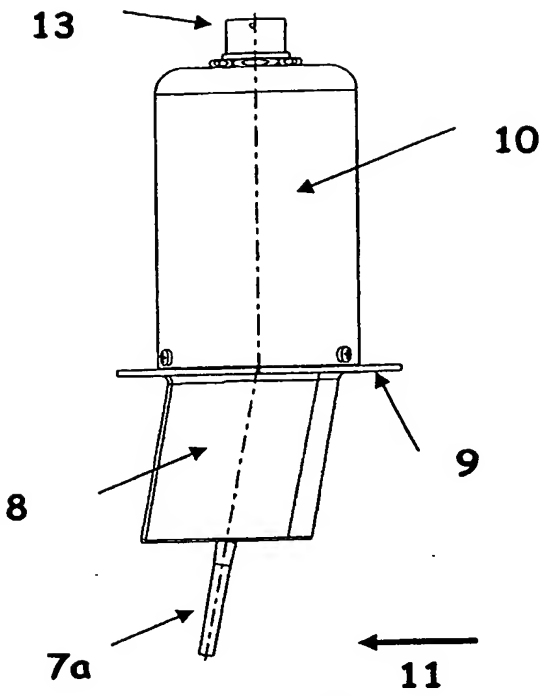

Figure 12a

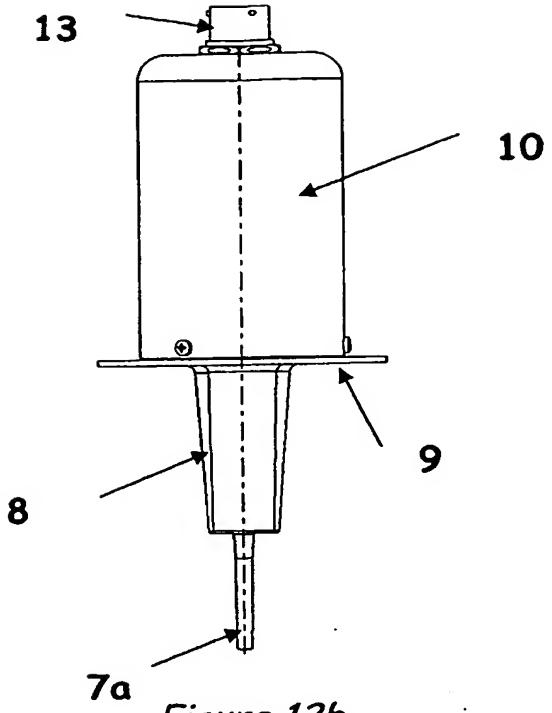

Figure 12b

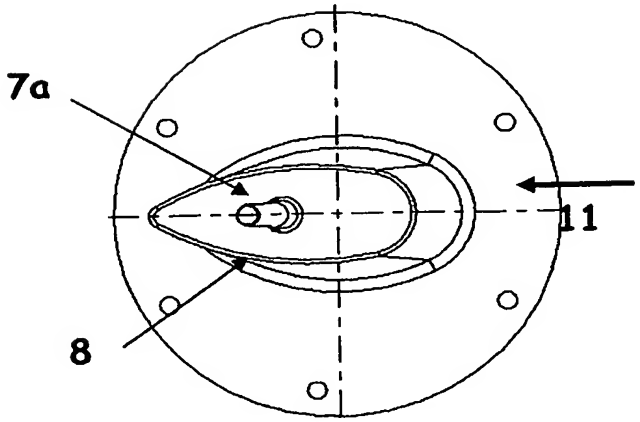

Figure 12c

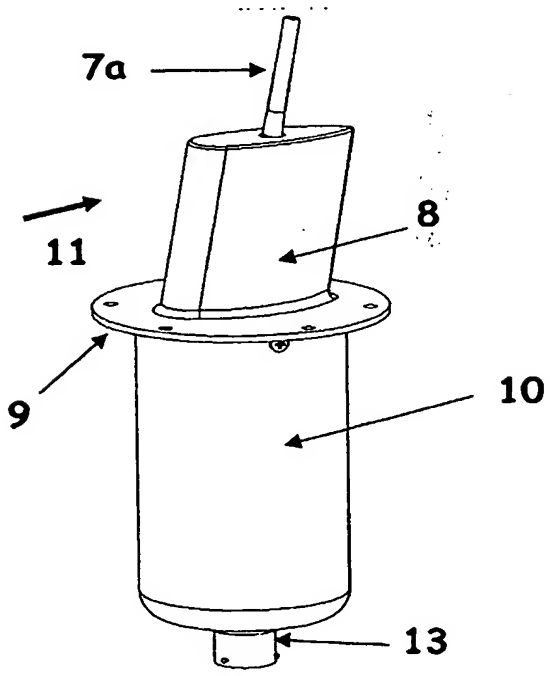

Figure 12d

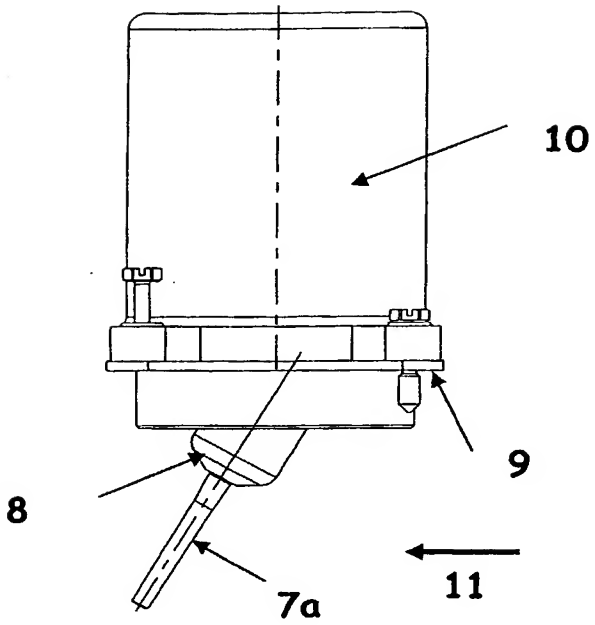

Figure 13a

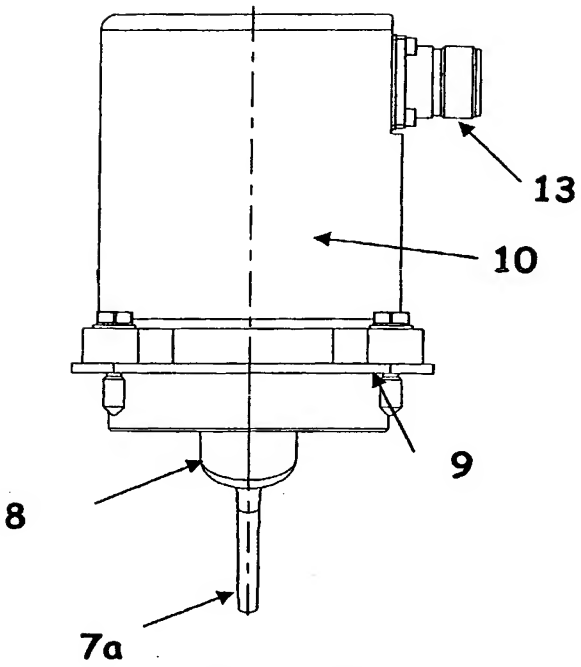

Figure 13b

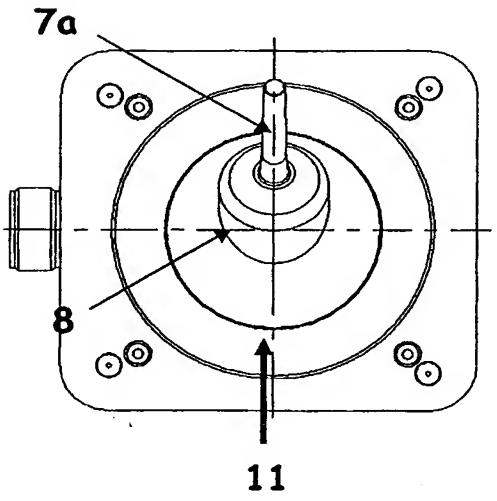

Figure 13c

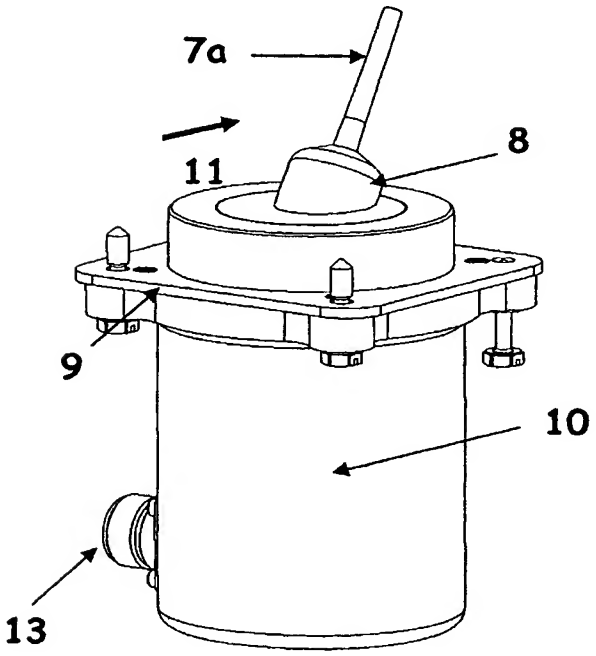

Figure 13d

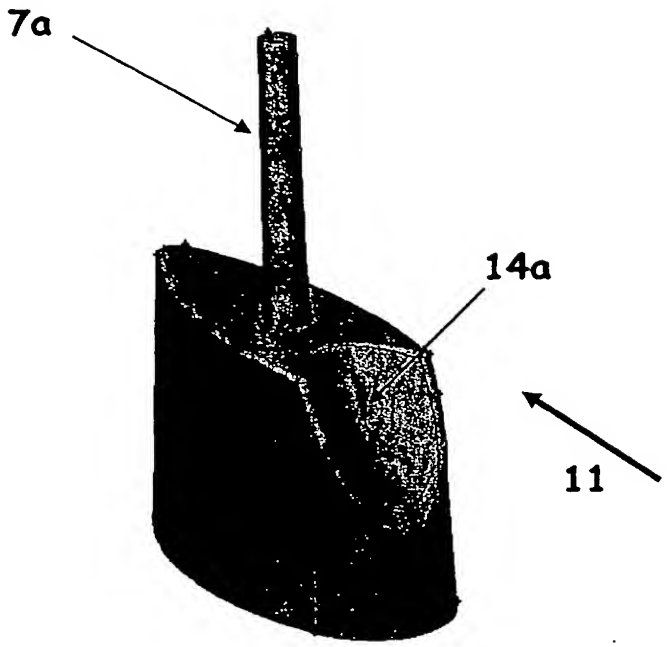

Figure 14a

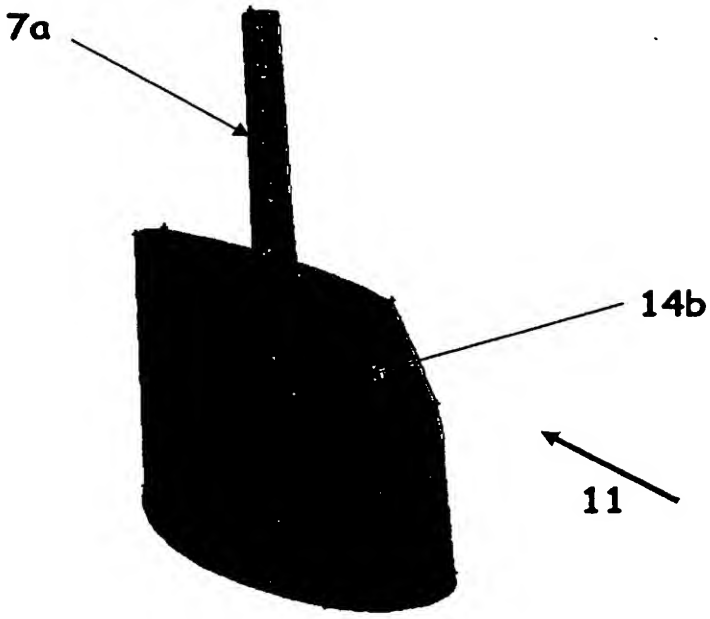

Figure 14b

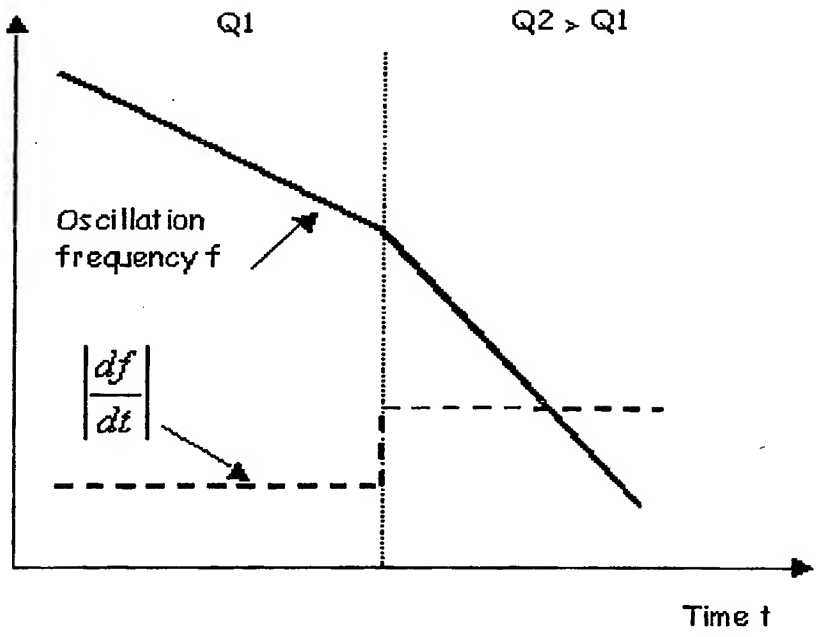

Figure 15a

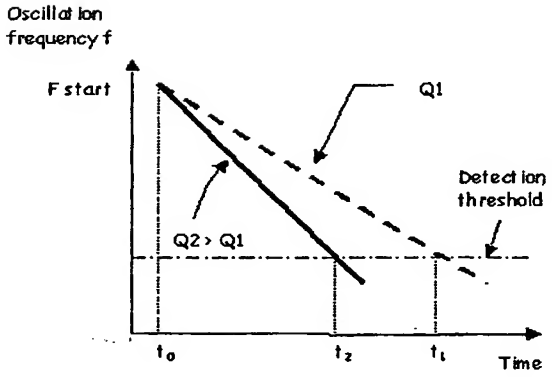

Figure 15b

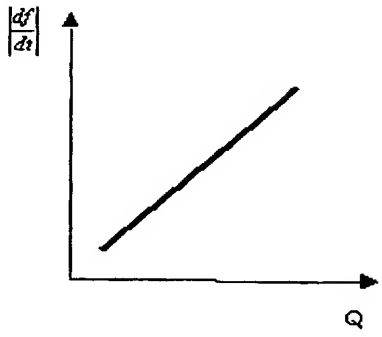

Figure 15c

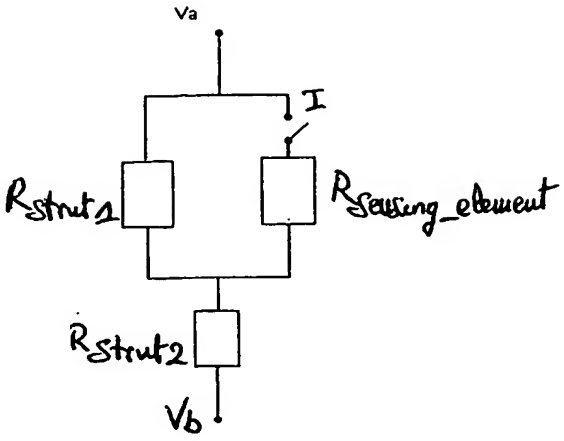

Figure 16a

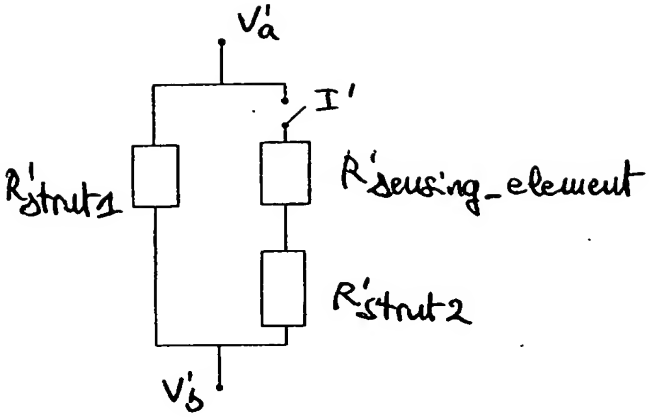

Figure 16b

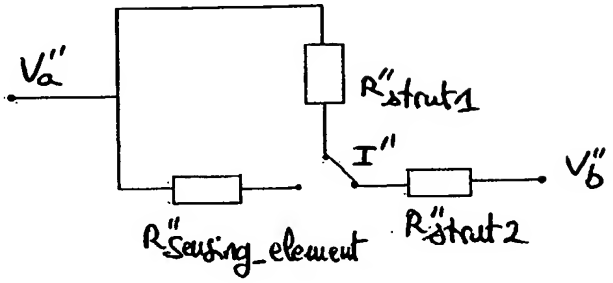

Figure 16c

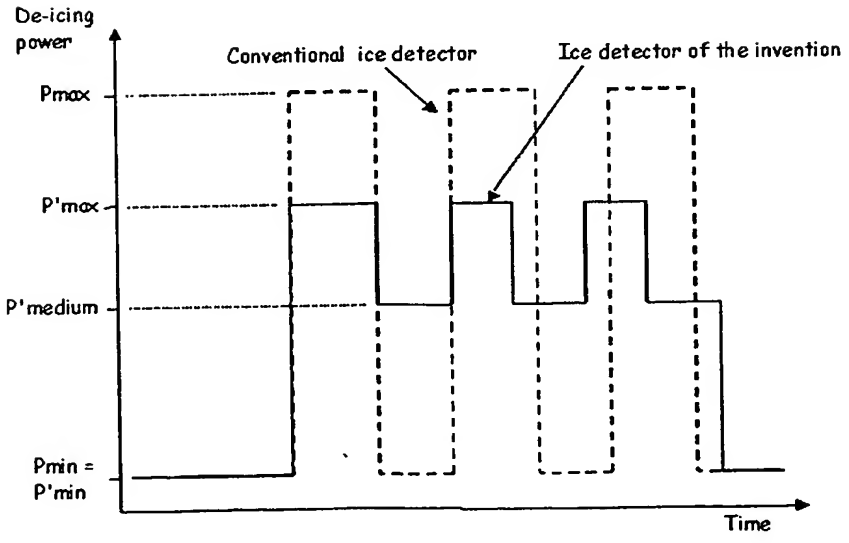

Figure 17